Structural Engineering and Mechanics, *Vol. 63, No. 6 (2017) 761-769*
DOI: https://doi.org/10.12989/sem.2017.63.6.761

Wavelet-based automatic identification method of axle distribution information

Ning-Bo Wang[1a], Wei-Xin Ren[*2] and Zhi-Wei Chen[3b]

[1]*School of Civil Engineering, Central South University, Changsha 410075, Hunan, China*
[2]*Department of Civil Engineering, Hefei University of Technology, Hefei 230009, Anhui, China*
[3]*Department of Civil Engineering, Xiamen University, Xiamen 361005, Fujian, China*

(Received October 15, 2016, Revised April 12, 2017, Accepted May 3, 2017)

Abstract. Accurately extracting the axle distribution information of a passing vehicle from bridge dynamic responses experiences a key and challenging step in non-pavement bridge weigh-in-motion (BWIM). In this article, the wavelet transformation is adopted and the wavelet coefficient curve is used as a substitute for dynamic response. The driving frequency is introduced and expanded to multi-axle vehicle, and the wavelet coefficient curve on specific scale corresponding to the driving frequency is confirmed to contain obvious axle information. On this basis, an automatic method for axle distribution information identification is proposed. The specific wavelet scale can be obtained through iterative computing, and the false peaks due to bridge vibration can be eliminated through cross-correlation analysis of the wavelet coefficients of two measure points. The integrand function that corresponds to the maximum value of the cross-correlation function is used to identify the peaks caused by axles. A numerical application of the proposed axle information identification method is carried out. Numerical results demonstrate that this method acquires precise axle information from the responses of an axle-insensitive structure (e.g., girder) and decreases the requirement of sensitivity structure of BWIM. Finally, an experimental study on a full-scale simply supported bridge is also conducted to verify the effectiveness of this method.

Keywords: dynamic strain responses; axle distribution information; automatic identification; wavelet coefficient; driving frequency; specific scale

1. Introduction

Axle information, including axle distance, number of axles and vehicle speed, plays an important role in vehicle load identification and bridge weigh-in-motion (BWIM) which has been commonly used in bridge safety monitoring for the merits of high durability, low cost, and no damage to the bridge deck (O'Brien *et al*. 2008, Lydon *et al*. 2016). The identification of axle information is a key process of BWIM, and it directly affects the application scope and testing accuracy of the BWIM system and guides its development.

When BWIM was firstly developed by Moses (1979), axle identification relied on connected facilities set on the road, such as reflective strips and third diagonal tube (Quilligan *et al*. 2002). Auxiliary facilities always have poor durability and are limited to provisional tests. Eventually, non-pavement axle detection was introduced (Mcnulty and O'Brien 2003, Xiao *et al*. 2006, Park *et al*. 2008, Hitchcock 2011, 2012) and contributed to the nothing-on-road BWIM system. In this system, the transducer is not directly set under vehicle load and has sufficient testing precision. It was widely adopted for several decades. Recently, visual system has been used for axle detection in the BWIM system (Lydon *et al*. 2016). It can provide axle configurations without disrupting the flow of traffic by using a roadside camera system placed perpendicular to the traffic flow.

According to the above analysis, the method of identifying axle information from bridge dynamic responses caused by a passing vehicle does not need additional devices and has an obvious advantage in economy and curability. This study extends the previous work to automatic identification of axle information from bridge dynamic responses in combination with wavelet transform.

In relation to the work developed in this paper, Kobayashi *et al*. (2004) used the traditional local peak detection method for axle detection. Their method is only suitable for dynamic responses with a high signal-to-noise ratio and obvious peaks, such as responses of orthotropic steel deck bridge, which has a sensitive component to vehicle axles, such as the bending-plate WIM system. Navid *et al*. (2013) investigated the axle information identification of different vehicles crossing a simply supported beam bridge with a 24.8 m span. The results of derivation and cross-correlation analysis differed greatly, especially for wheelbase identification. In addition, when two peaks are close, denoising the early signal will cause the loss of peak information.

Wavelet-transform-based signal processing is proved to be efficient for damage detection (He *et al*. 2014, Liu *et al*. 2015) and physical parameter identification (Wang *et al*. 2014). It is also suitable for axle information identification

∗Corresponding author, Professor
E-mail: renwx@hfut.edu.cn
[a]Assistant Professor
E-mail: wangnb@csu.edu.cn
[b]Associated Professor
E-mail: cezhiwei@xmu.edu.cn

ISSN: 1225-4568 (Print), 1598-6217 (Online)

and can deal with the disadvantages of the traditional method. On the basis of the time-frequency localizing characteristic of wavelet transform, continuous wavelet transformation is applied to the dynamic response, and a wavelet coefficient curve is extracted to replace the original signal, which reduces the noise and makes the peak obvious. Chatterjee *et al*. (2006) applied wavelet transform to axle information identification firstly. The wavelet coefficient curve extracted from bridge dynamic response are used to identify the axle information. In addition, influences of different wavelet basis functions and scaling coefficients were studied. And rbio2.4 was considered as an ideal wavelet basis for axle information identification. Sakayanagi *et al*. (2008) used wavelet transform method to increase the accuracy of axle weight and reduce the number of the measurement points for orthotropic plate bridge. Lechner *et al*. (2010) used a 7.5 m span simply supported plate bridge and a 12.6 m span plate bridge with elastomeric bearings as study cases to identify the axle information by extracting wavelet coefficient curve from the dynamic response of crack width.

With the use of the wavelet coefficient as an alternative to dynamic response in these methods, the interference of testing noise is reduced and the application range is expanded somewhat. However, the subjectivity of wavelet coefficient selection is an ongoing problem, the wavelet coefficient under different scales always results in inconsistent peak value and axle information.

In this study, a wavelet-based automatic identification method of axle distribution information is proposed. Together with the bridge responses of different sections caused by passing vehicle, a series of discrete wavelet transform was introduced to obtain the wavelet coefficient curve on different wavelet scales. Some new skills such as iterative computation and cross-correlation analysis are adopted for the automatic identification of axle distribution information. The driving frequency produced by passing vehicle, as well as the specific scale of wavelet are introduced and established through iterative computation. Then, the wavelet coefficient curves for different measurement points are chosen based on this specific scale. Through cross-correlation analysis on the positive part of the above wavelet coefficient curves, the integrand curve is extracted by using a maximum interrelation algorithm, which could eliminate the false peaks due to bridge vibration and obtain exactly identical results.

This paper is organized as follows: Section 2 introduces the concept of driving frequency by passing vehicles and the specific scale coefficient of wavelet transform. Section 3 presents the theoretical approaches and processes of automatic identification of axle information from bridge dynamic responses. Section 4 shows a numerical example of vehicle-bridge coupling vibration to verify the method of this article. Section 5 describes an experimental test used to illustrate the feasibility of the proposed method. Finally, some conclusions are presented in Section 6.

2. Preliminary remarks

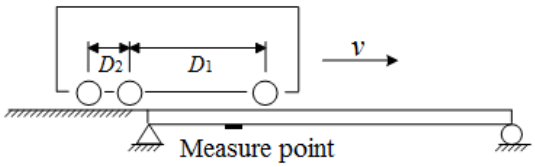

Fig. 1 Three-axle vehicle crossing a bridge

Preliminary insights into the driving frequency and wavelet scale provide hints for the automatic identification technique described in Section 3.

When the wavelet transform is performed on bridge dynamic responses, only the wavelet coefficient of a specific scale can represent the vehicle axle information well, and this specific scale is always decided by the driving frequency of passing vehicle. The frequency components of bridge vibration response induced by passing vehicles mainly include two types: (1) free vibration frequency of bridge and (2) driving frequency related to vehicle loading, which is determined by the speed and wheelbase, among others. When identifying axle information, driving frequency is the effective component, and bridge vibration is considered as interference.

2.1 Driving frequency of passing traffic

The driving frequency of a single-axle vehicle or an equivalent single-axle vehicle (when the ratio of the wheelbase to the length of the span is small) uniformly passing bridge is described as v/L (with the circle frequency $2\pi v/L$) by Yang *et al*. (2004, 2005), where v and L are the speed and the length of the span, respectively. The similarly expression is also used by He and Zhu (2016) when studying the load-induced response and damage localization. For small-span and medium-span bridges (Fig. 1), as well as the secondary system of large-span bridges, the vehicle cannot be considered a single-axle system because the wheelbase is close to the bridge span. In this case, the driving frequency should be determined according to the speed and the wheelbase, among other factors.

Fig. 1 shows a three-axle vehicle crossing a bridge with uniform speed v, where D_1 and D_2 are the wheelbases of vehicle. Assume Δt_1 denotes the time interval of the first and the second axles crossing the section of the measure point, Δt_2 denotes the time interval of the second and the third axles crossing the same cross-section of the bridge, and on the same for other axles. the expressions are as follows

$$\Delta t_1 = \frac{D_1}{v} \tag{1}$$

$$f_1 = \frac{1}{\Delta t_1} = \frac{v}{D_1} \tag{2}$$

$$\Delta t_1 = \frac{D_2}{v} \tag{3}$$

$$f_2 = \frac{1}{\Delta t_2} = \frac{v}{D_2} \tag{4}$$

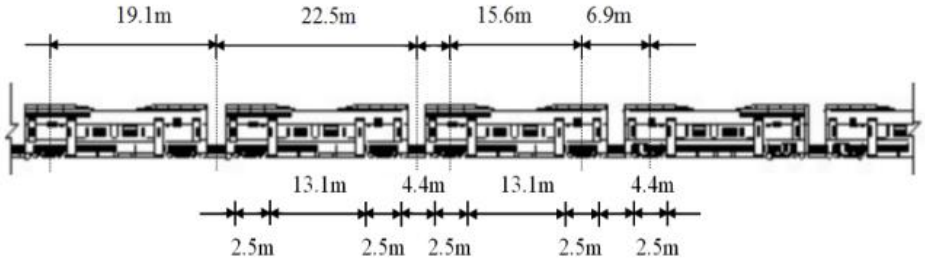

Fig. 2 Details of the high-speed train

From the above statement, it can be seen that only one driving frequency exists for the vehicle with two axles, and multiple driving frequencies exist for the vehicle with more than two axles. When the speed is constant, a short wheelbase corresponds to a high excitation frequency. And for the case of two or three axles close to each other, these axles can be seen as a combined axle.

2.2 Specific scale coefficient

The relationship between the wavelet transform scale and frequency is given by

$$scale = \frac{f_0 \times F_s}{F_a} \tag{5}$$

where *scale* denotes the wavelet transform scale coefficient, f_0 denotes the center frequency of the wavelet basis function, F_s represents the sampling frequency of the signal, and F_a is the frequency of interest. On the basis of Eq. (5), the wavelet transform scale coefficient is determined by the joint effect of the center frequency f_0, the sampling frequency F_s, and the interested frequency F_a. When the f_0 and F_s are fixed constant, *scale* is inversely proportional to F_a.

Multi-scale wavelet transform is performed on dynamic response to extract the time-domain information reflected by different scale coefficients. Choosing a proper scale coefficient is important for extracting wavelet coefficient curve. A large scale coefficient will cause few peaks in wavelet coefficient curve and lead to the loss of the effective information, whereas a small scale coefficient corresponding to high frequency will lead to excessive peaks. The proper scale coefficient can be determined by the driving frequency. For the case of multiple axles, the maximum driving frequency F_a=max(f_1, f_2,…) is used to determine the scale coefficient. The use of maximum driving frequency enables the wavelet coefficient curve to contain all the peaks related to the axles.

The measured strain data (Chen *et al*. 2016) when a high-speed train crosses the track beam of Tsing Ma Bridge are used to investigate the peak features of the wavelet coefficient curve at different frequencies. The high-speed train consists of 8 carriages and 16 bogies. The details of this high-speed train are shown in Fig. 2. Fig. 3 shows the dynamic response when the train crosses the bridge at the speed of 130 km/h, and the strain data is recorded with sampling frequency 51.2 Hz. The distances between two close bogies are 6.9 and 15.6 m, respectively. Thus, the

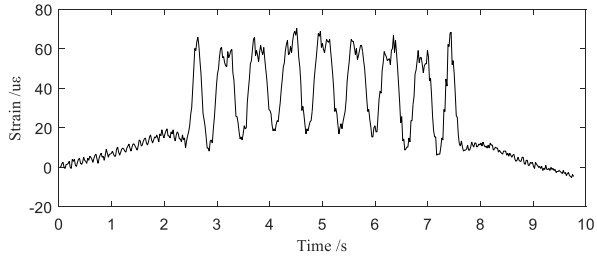

Fig. 3 Dynamic response when the high-speed train crosses the bridge

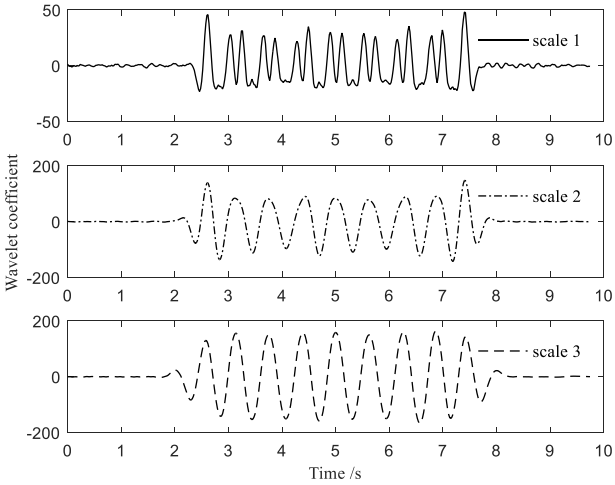

Fig. 4 Wavelet coefficient curves of different scale

equivalent distance for two close bogies is 22.5 m. On the basis of Eqs. (1)-(4), the driving frequencies are f_1=36/6.9 =5.2 Hz, f_2=36/15.6=2.3 Hz, and f_3=36/22.5=1.6 Hz. A wavelet basis function rbio 2.4 is chosen for the analysis, basing on Eq. (5) the scale1=9 corresponding to f_1, scale2 =20.3 corresponding to f_2, and scale3=28.6 corresponding to f_3 are used for wavelet transform and wavelet coefficient extraction. Results are shown in Fig. 4.

The original signal in Fig. 3 contains obscure peak information and is strongly influenced by the high frequency noise. From wavelet coefficient extracted by *scale*1, the identified distance of adjacent bogies are 15.9, 7.9, 14.4, 7.9, 15.1, 7.9, 15.1, 7.9, 15.1, 7.9, 15.1, 7.9, 15.9, 7.2 and 15.1 m, which are close to the true values of 15.6 m and 7.9 m. From wavelet coefficient curves by *scale*2 and *scale*3, only few peak points can be obtained for the two close bogies are considered as one whole. The identified distance of adjacent bogies are 18.3, 21.8, 25.3, 19.7, 22.5, 25.3, 21.1, 18.3 m when using *scale*2, and 19.7, 22.5, 22.5,

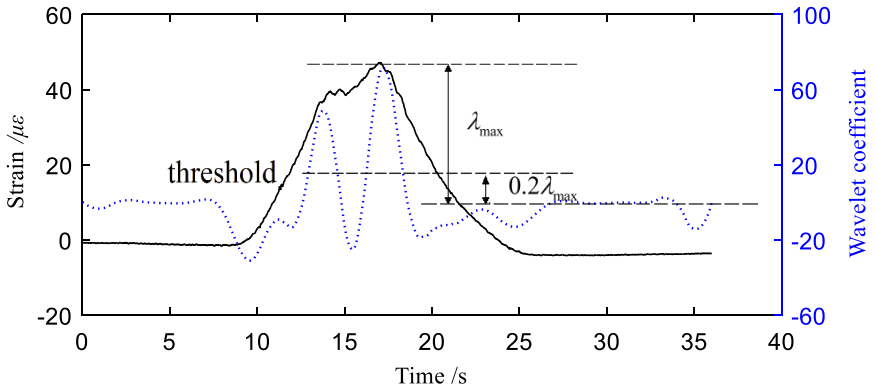

Fig. 5 Calculation of the number of peaks and the threshold

21.8, 22.5, 23.2, 21.8, 19.7 m when using *scale*3. The 'axle distance' results from *scale*3 are closer to the true values of 19.1 and 22.5 than the results from *scale*2.

In light of the above results, the wavelet coefficient curves with different scales present different peak information and amplitudes. The wavelet coefficient curves with specific scale determined by driving frequency can remove the interference by noise and make the peak associated with axles obvious. Considering the case of a vehicle crossing the bridge at a uniform speed, the driving frequency is existent and unique but cannot be determined subjectively.

3. Automatic axle information identification method

3.1 Iterative computing and axle identification

The previous section stated that the driving frequency is vital for axle information identification. However, the measured signal when the vehicle crosses the bridge fails to contain enough information. Thus, spectrum analysis is unable to obtain the driving frequency. On the basis of the idea that axle information determines the driving frequency and that the driving frequency can be used to extract the proper wavelet coefficient curve for axle information identification, an iterative computing method for axle information identification is proposed. The related steps are as follows:

(1) The range of the driving frequency is determined.

The range of driving frequency depends on the speed and wheelbase, and is expressed by

$$f_{max} = v_{max}/D_{min} \tag{6}$$

$$f_{min} = v_{min}/D_{max} \tag{7}$$

where v_{max} and v_{min} denote the maximum and minimum speed limits, respectively, D_{max} and D_{min} denote the maximum and minimum wheelbases, respectively. For the BWIM of the railway bridge, these parameters can be determined according to the relevant design code.

(2) The initial driving frequency is computed.

The range of the driving frequency is uniformly divided as follows

$$f = [\, f_{max} \quad f_{max} - \Delta f \quad f_{max} - 2\Delta f \quad \cdots \quad f_{min} \,] \tag{8}$$

$$\Delta f = \frac{f_{max} - f_{min}}{n} \tag{9}$$

where n is an integer that should be as big as possible.

In practical application, the driving frequencies in Eq. (8) is chosen to extract the wavelet coefficient curve. When the driving frequency is high, the wavelet coefficient curve presents burr. When the driving frequency is low, the wavelet coefficient curve is too smooth and unable to reflect the axle information. Therefore, selecting a proper driving frequency is important. The number of peaks of the wavelet coefficient curve extracted by using the proper driving frequency is equal to the number of axles. A vehicle usually has less than seven axles. Thus, the maximum number limit of peaks (denoted by N_{max}) should be set. When the driving frequency is used to extract the wavelet coefficient curve, its peaks are more than N_{max}, and this driving frequency is regarded as improper. Then the next driving frequency will be used until the proper driving frequency is found. The proper threshold value equal to 20% of the maximal amplitude is set, and the number of peaks is established by comparing the peak value and the threshold value, as shown in Fig. 5.

After the range of the driving frequency noted as vector $\{\boldsymbol{f}\}$ has been established, each value is selected as the initial driving frequency in turn. And its reasonableness is evaluated by calculation until the accurate driving frequency and the axle information are acquired. This entire task is performed on MATLAB platform. The corresponding calculation flowchart is shown in Fig. 6.

$\{\boldsymbol{f}\}_j$ represents the j^{th} supposed initial frequency when the axle information is unknown, $\{scale\}_j$ is the corresponding wavelet scale.$\{v\}_j$ and $\{d\}_j$ are the calculated vehicle velocity and axle distance based on $\{\boldsymbol{f}\}_j$ and $\{scale\}_j$. $\{\boldsymbol{f}'\}_j$ and $\{scale'\}_j$ are extracted from the calculated axle information. Lastly, $\{scale\}_N$,$\{v\}_N$ and $\{d\}_N$ are the most proper value obtained through the whole iterative calculation.

3.2 Eliminating interference peaks

Bridge vibration response induced by vehicles crossing

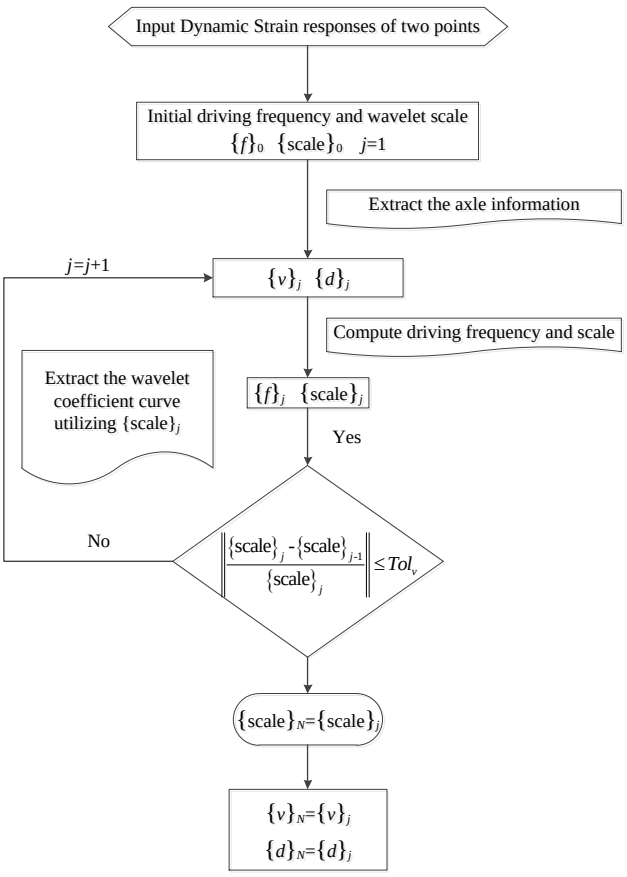

Fig. 6 Flowchart of the axle information identification

the bridge contains bridge natural frequency and driving frequency. For the bridge with structural components that are sensitive to the axle, driving frequency is dominant, and the peaks related to the axle are clear and can be extracted easily. The bridge vibration response is contaminated by noise, which causes excess peaks. In this case, wavelet transform technique can clarify the peaks of the wavelet scale coefficient curve, but it fails to remove the interference due to bridge vibration when driving frequency and bridge free vibration frequency are close. Removing the induced interference is important because it ensures that axle information can be extracted easily from the obscure original signal.

Assuming the wavelet scale coefficient curve that corresponds to the points at two different cross sections as $f(t)$ and $g(t)$, $t_1<t<t_2$, t_1, t_2 denote the beginning time and ending time of the signal, respectively. Only the peaks whose values are positive are taken into consideration. The related expressions are given as

$$X(t)=\begin{cases}1, & t_1<t<t_2\\ 0, & \text{else}\end{cases} \tag{10}$$

$$F(t)=f^{+}(t)X(t) \tag{11}$$

$$G(t)=g^{+}(t)X(t) \tag{12}$$

$$C(\tau)=\int F(t-\tau)G(t)dt \tag{13}$$

Where $X(t)$ is an auxiliary constructor used for extending other functions in time domain. $f^{+}(t)$ and $g^{+}(t)$ represent the positive part of $f(t)$ and $g(t)$ respectively, which change the negative value of original function to zero, and are used for eliminating the disturbance of valley value in correlation analysis.

Even though the interference due to bridge vibration exists, the peak information induced by vehicle loading is dominant. Thus, $\Phi(t)=F(t-\tau_0)G(t)$ when $C(\tau)$ is maximum can be used for axle information identification. The correlation between the effective peaks of $F(t)$ and $G(t)$ ($\tau=\tau_0$) is great, while that between false peaks is weak. Multiplication is used to retain and enlarge useful peaks and reduce false peaks, thereby eliminates the interference due to the bridge vibration and extracts axle information from obscure dynamic response. This idea of removing false peaks will be verified by numerical examples and experimental studies in Section 4 and Section 5.

4. Numerical study

A simply supported beam bridge on which a three-axle vehicle crosses is used as a case study. The parameters of the bridge are as follows: span L=16 m, distance between neutral axis and the bottom of beam L_a=0.8 m, bending rigidity EI=4.36×10^9 Nm^2, linear density P_a=1.07×10^4 kg/m, damping coefficient ξ=0.02, and first bending frequency f_1=3.91 Hz. Bakht (2009) maintains that the dynamic response at the points close to the support is more sensitive for the beam bridge. Accordingly, the dynamic responses of points at 1/8 L (Point 1, noted as P_1) and 7/8 L (Point 2, noted as P_2) are adopted to extract axle information, and the measured points are installed at the bottom of the girder.

The details of the vehicle can be found in Ref. (Zhu *et al*. 2005). The wheelbase between the first and second axles is 3.66 m, and the wheelbase between the second and third axles is 6.20 m. A total of 10 degrees of freedom, including vehicle body vertical vibration, rotation, and wheel vertical vibration, is considered. For this vehicle and the bridge model, the patch contact of the tire and the road surface is simplified as a point contact. If the surface classification is poor, then this contact condition will overestimate the dynamic deflection of the bridge and magnify the effect of road surface roughness (Yin *et al*. 2011). Thus, a good roughness grade such as Road Classes A (ISO 8608 1995) is assumed in this numerical study. Within the MATLAB framework, Newmark-β method is utilized to compute the dynamic strain signal, and the computing frequency is 500 Hz. The simulated dynamic strains are used to detail the procedure of the proposed axle information identification method.

The identified results of velocity and wheelbases from responses under different driving speeds are listed in Table 1. The results verify that this method is feasible for the extraction of axle information from the obscure original signal, even when the driving frequency is close to the bridge natural frequency and in cases with a high driving speed.

Table 1 Identified results of axle information of numerical case

No.	Speed (m/s)		Wheelbase D_1 (m)		Wheelbase D_2 (m)	
	True value	Identified value	True value	Identified value	True value	Identified value
1	2	2.03	3.66	3.86	6.20	6.25
2	4	4.05		3.87		6.22
3	6	6.01		3.84		6.17
4	8	8.02		3.83		6.19
5	10	10.06		3.75		6.24
6	12	11.90		3.50		6.12
7	14	14.85		4.36		6.62
8	16	16.17		4.08		5.73
9	18	18.92		4.43		6.39
10	20	21.2		4.45		6.40
11	22	22.22		4.64		5.71
12	24	23.72		3.75		6.25
13	26	24.90		3.34		5.63
14	28	28.17		3.66		6.25
15	30	29.85		3.64		6.15
16	32	31.41		3.58		6.09
17	34	33.33		3.53		6.07
18	36	35.50		3.62		6.18

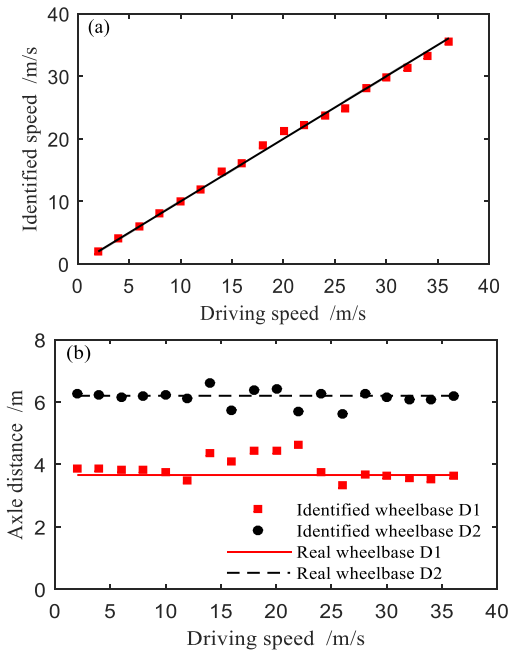

Fig. 7 Axle information identification of the different scenarios. (a) speed and (b) wheelbase

The identified velocities that correspond to the speeds of 2 m/s, 4 m/s,…, 36 m/s are shown in Fig. 7(a), which shows that the identified velocities agree fairly well with the real value. Fig. 7(b) shows the identified wheelbase results of different scenarios related to different speeds. As shown in Fig. 7(b), the result for the wheelbase (3.66 m) between the first and the second axles is not as accurate as that for the wheelbase (6.20 m) between the second and the third axles. A relatively large error exists when the speed is 14 m/s-24 m/s because the driving frequency is close to the bridge natural frequency, which causes a larger bridge vibration interference and influences the identified results.

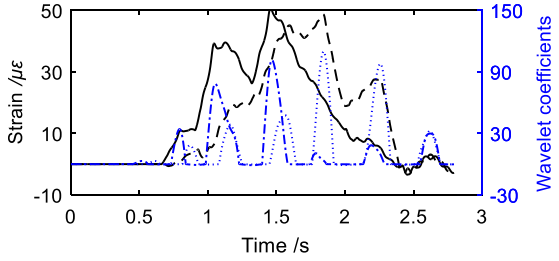

-:dynamic response of P_1, --:dynamic response of P_2,
—·:wavelet coefficient of P_1, ··:wavelet coefficient of P_2

Fig. 8 Dynamic strain responses and its wavelet coefficients under the specific scale of P_1 and P_2

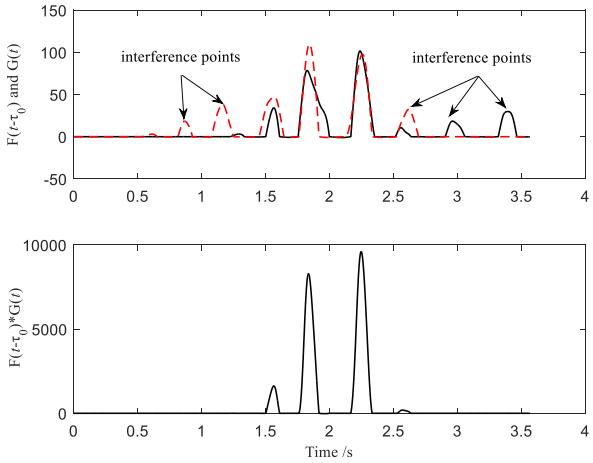

Fig. 9 Positive part of coefficient curves and the integrand function of the maximum interrelation

Then the scenario that corresponds to the speed of 15 m/s is studied. The resulting driving frequencies are 4.09 Hz and 2.42 Hz by the two groups of adjacent axles, respectively, and the former is quite close to the bridge natural frequency of 3.91 Hz. The proposed method is used to extract the wavelet coefficient curves of a specific scale from the dynamic strain response of P_1 and P_2. The wavelet coefficient and its corresponding initial signal of two points are shown in Fig. 8, which shows that the wavelet coefficient of a specific scale can be effective for denoising and making peaks obvious.

For the driving frequency that is close to the bridge natural frequency, from Fig. 8, it can be determined that the extracted wavelet coefficient contains the effective peaks that correspond to the axle and the false peaks due to bridge vibration as well. In this situation, cross-correlation analysis on the positive part of wavelet coefficient curve can be used. The state of two coefficient curves when the cross-correlation function is maximum and the convolution operation result on integrand function are shown in Fig. 9. It is obviously that the interference of false peaks due to bridge vibration is removed.

5. Experimental verification

Fig. 10 Huangkou Bridge

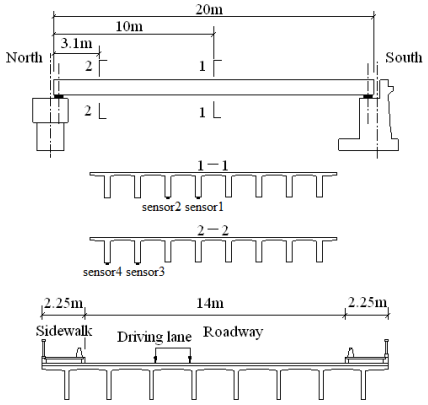

Fig.11 Arrangement of measuring points

The Huangkou Bridge, which is located in Huangshan city, Anhui Province of China, is a multi-span simply supported beam bridge (Fig. 10). The bridge is 20 m long and 18.5 m wide. The driving way is 14 m wide, and the sideway is 2.25 m wide. The bridge consists of eight T-shaped girders. The measured first bending frequency is 3.06 Hz. This real bridge is used to verify the feasibility of the proposed method. The measured cross-sections and arrangement of measuring points are shown in Fig. 11.

The vehicle drives through the bridge using the second lane. The tested vehicle has three axles, the wheelbase between the first and second axles is 4.0m, and the wheelbase between the second and third axles is 1.4 m. The axle weights are 89.4, 179.2, and 178.2 kN. The speeds are controlled at 5, 10, 20, and 40 km/h. As shown in Fig. 12, the measured dynamic responses demonstrate that a high speed corresponds to a strong interference because the driving frequency becomes closer to the natural frequency of the bridge.

The proposed method automatically determines the specific scale and identifies the axle information. The identified results of four scenarios that correspond to four different speeds are shown in Fig. 13, which shows that the peaks related to axles are obvious. For the scenarios that correspond to the speeds of 5, 10, and 20 km/h, the interference is weak. Thus, no false peaks are present in the wavelet coefficient curves. The low peaks of Figs. 13(a)-(c) are related to the first axle, while the high peaks are related to the center of the second and third axles. The theoretical distance between two peaks is 4.7 m. The second and third axles are seen as a whole when performing axle information identification. But for the scenario that corresponds to the lowest speed of 5 km/h, the frequency due to the combined

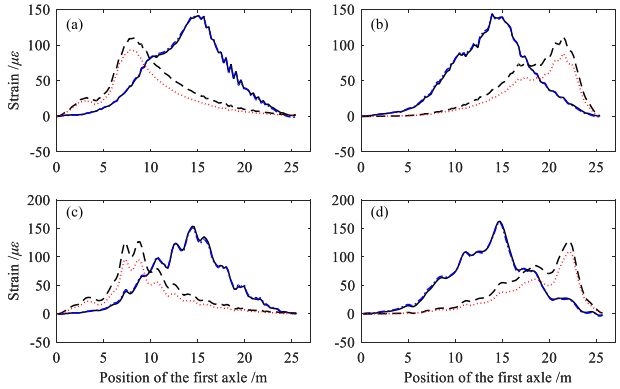

Fig. 12 Strain responses of sensor1 (-), sensor2 (—·), sensor3 (--) and sensor4 (··) by passing vehicle at different speed. (a) *v*=5 km/h, (b) *v*=10 km/h, (c) *v*=20 km/h and (d) *v*=40 km/h

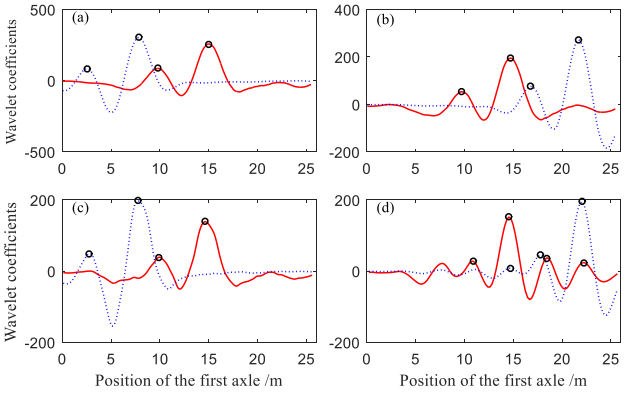

Fig. 13 Wavelet coefficient curves of sensor2 (red solid line) and sensor3 (blue dotted line) at the specific scale ("o" marks the peaks).(a) *v*=5 km/h, (b) *v*=10 km/h, (c) *v*=20 km/h and (d) *v*=40 km/h

axle can also be identified. The results of cross-correlation analysis on the combined axle are shown in Fig. 14.

For the speed of 40 km/h, the driving frequency is 80% of the bridge natural frequency. The wavelet coefficient curve related to the specific scale contains the peaks associated with axles and also the false peaks due to bridge vibration. Therefore, the cross-correlation operation is performed on the two wavelet coefficient curves and the integrand function when the cross-correlation function is maximum is used to remove the false peaks. The identified results of four scenarios are summarized in Table 2. The identified results agree well with the true values, which means that the proposed method performs axle identification with high accuracy.

The field test verifies that the proposed method is feasible for axle information identification from the obscure dynamic response when noise due to bridge vibration exists. Therefore, this study can enlarge the application range of BWIM and increase the accuracy as well.

6. Conclusions

This work proposed a new approach for extracting the

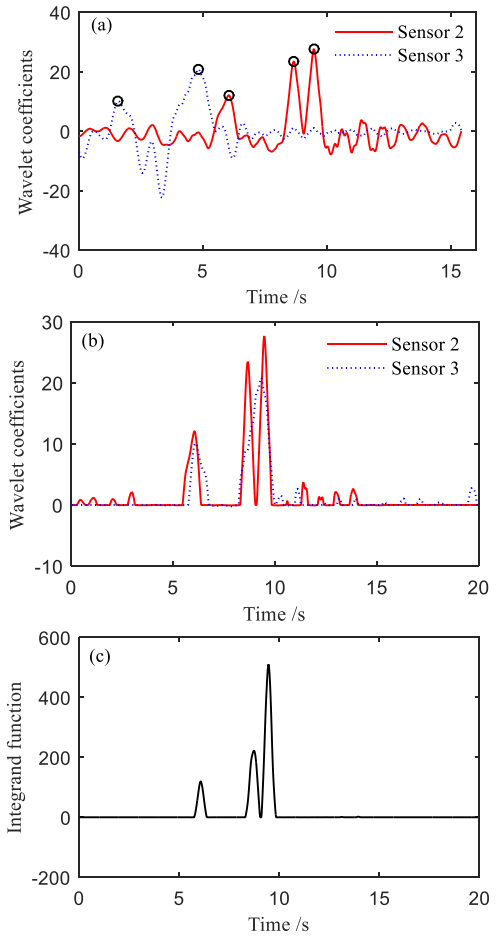

Fig. 14 (a) wavelet coefficient curves of two sensors, (b) the maximum cross-correlation state of positive part of wavelet coefficient and (c) integrand function of cross-correlation analysis

axle information of passing vehicle based on wavelet transform, and the wavelet coefficient curve is adopted to replace the dynamic response for axle identification. The concept of driving frequency is introduced to select the wavelet scale, and the relationship between driving frequency and axle information is studied. Then the automatic axle information identification is developed by iterative computing to avoid subjective selection. The cross-correlation of the wavelet coefficients on two points of different sections is analyzed, and the integrand function that corresponds to the maximum value of the cross-correlation function is used to identify the peaks caused by axles. This function eliminates the false peaks due to the interference caused by the bridge vibration and extracts axle information from obscure dynamic response.

A numerical simulation of axle information identification and a full-scale study case of a vehicle passing through a simply supported bridge are used to illustrate the procedure of the proposed method. The feasibility of identifying the axle information from obscure dynamic response of beam structures is verified. The proposed method is also proved to decrease the sensitivity requirement of the structural components of a bridge for BWIM, thereby expands the application range of BWIM.

Table 2 Axle information identified results from responses of Huang kou Bridge

No	Driving frequency		Speed (km/h)		Wheelbase D_1* (m)		Wheelbase D_2 (m)	
	Combine axle	Separat axle	True value	Identified value	True value	Identified value	True value	Identified value
1	1.18	0.35	5.95	5.66	4.0	4.05	1.4	1.26
2	1.93	0.58	9.75	9.66		4.85	/	/
3	3.80	1.13	19.2	19.0	4.7	4.69	/	/
4	7.63	2.28	38.5	35.6		4.83	/	/

*D_1: Represent the distance between axle 1 and 2 for No. 1; and the distance between axle 1 and the center of axle 2 and 3 for No. 2-4.

Acknowledgments

This work is support by National Natural Science Foundation of China (NSFC) with Grant no. 51508576. This support is gratefully acknowledged.

References

Bakht, B., Mufti, A. and Jaeger, L.G. (2009), "Bridge weighing-in-motion systems and their use in SHM of bridges", *Proceeding of the 4th International Conference on Structural Health Monitoring of Intelligent Infrastructure*, Zurich, Switzerland, July.

Chatterjee, P., O'Brien, E.J., Li, Y. and González, A. (2006), "Wavelet domain analysis for identification of vehicle axles from bridge measurements", *Comput. Struct.*, **84**(28), 1792-1801.

Chen, Z.W., Cai, Q.L. and Li, J. (2016), "Stress influence line identification of long suspension bridges installed with structural health monitoring systems", *Int. J. Struct. Stab. Dyn.*, **16**(04), 1640023.

European Commission (2001), "Weight-in-motion of axles and vehicles for Europe (WAVE)", General Report, Paris, LCPC.

European Commission (2001), "Weight-in-motion of axles and vehicles for Europe (WAVE)", Report of Work Package 1.2-Bridge WIM Systems, University College Dublin, Ireland.

He, W.Y. and Zhu, S. (2016), "Moving load-induced response of a damaged simply-supported beam and its application in damage localization", *J. Vib. Control*, **22**(16), 3601-3617.

He, W.Y., Zhu, S. and Ren, W.X. (2014), "A wavelet finite element-based adaptive-scale damage detection strategy", *Smart Struct. Syst.*, **14**(3), 285-305.

Hitchcock, W.A., Salama, T., Zhao, H., Callahan, D., Toutanji, H., Richardson, J. and Jackson, J. (2011), "Expanding portable BWIM technology", UTCA Project No. 08204, Tuscaloosa, AL, USA.

Hitchcock, W.A., Uddin, N., Sisiopiku, V., Salama, T., Kirby, J., Zhao, H. and Richardson, J. (2012), "Bridge Weigh-in-Motion (BWIM) System Testing and Evaluation", UTCA Project No. 07212, Tuscaloosa, AL, USA.

ISO 8608 (1995), Mechanical vibration-road surface profiles-reporting of measured data.

Kobayashi, Y., Miki, C. and Tanabe, A. (2004), "Longterm monitoring of traffic loads by automaticreal timeweigh in motio", *J. Struct. Mech. Earthq. Eng.*, **69**(773), 99-111.

Lechner, B., Lieschnegg, M., Mariani, O., Pircher, M. and Fuchs, A. (2010), "A wavelet-based bridge weigh-in-motion system", *Int. J. Smart Sens. Intel. Syst.*, **3**(4), 573-591.

Liu, J.L., Wang, Z.C., Ren, W.X. and Li, X.X. (2015), "Structural time-varying damage detection using synchrosqueezing wavelet transform", *Smart Struct. Syst.*, **15**(1), 119-133.

Lydon, M., Taylor, S.E., Robinson, D., Mufti, A. and O'Brien, E.J. (2016), "Rencent development in bridge weigh in motion", *J. Civil Struct. Hlth. Monit.*, **6**(1), 69-81.

Mcnulty, P. and O'Brien, E.J. (2003), "Testing of bridge weigh-inmotion system in a sub-Arctic climate", *J. Test. Eval.*, **31**(6), 497-506.

Moses, F. (1979), "Weigh-in-motion system using instrumented bridges", *Tran. Eng. J.*, ASCE, **105**(3), 233-249.

O'Brien, E.J., Znidaric, A. and Ojio, T. (2008), "Bridge weigh-in-motion: Latest developments and applications worldwide", *Proceeding of the International conference on heavy vehicles incorporating heavy vehicle transport technology and weigh-in-motion*, Paris, France, May.

Park, M.S., Jo, B.W., Lee, J.W. and Kim, S.K. (2008), "Development of PSC I girder bridge weigh-in-motion system without axle detector", *J. Korean Soc. Civil Eng.*, **28**(5A), 673-683.

Quilligan, M., Karoumi, R. and O'Brien, E.J. (2002), "Development and testing of a 2-dimensional multi-vehicle bridgeWIM algorithm", *Proceeding of the 3rd international conference on weigh-in-motion (ICWIM3)*, Orlando, USA, May.

Sakayabagi, H., Sasaki E., Theeraphong C., Suzuki, K., Ishikawa, Y., Yamada, H. and Katsuchi, H. (2007), "Analysis of axle position information from strain history data with long influence lines", *Psychophys.*, **9**(3), 318-333.

Wang, C., Ren, W.X., Wang, Z.C. and Zhu, H.P. (2014), "Time-varying physical parameter identification of shear type structures based on discrete wavelet transform", *Smart Struct. Syst.*, **14**(5), 831-845.

Xiao, Z.G., Yamada, K., Inoue, J. and Yamaguchi, K. (2006), "Measurement of truck axle weight by instrumenting longitudinal ribs of orthotropic bridge", *J. Bridge Eng.*, **11**(5), 526-532.

Yang, Y.B. and Lin, C.W. (2005), "Vehicle-bridge interaction dynamics and potential applications", *J. Sound Vib.*, **284**(1-2), 205-226.

Yang, Y.B., Lin, C.W. and Yan, J.D. (2004), "Extracting the bridge frequencies from the dynamic response of a passing vehicle", *J. Sound Vib.*, **272**(3-5), 471-493.

Yin, X.F., Fang, Z. and Cai, C.S. (2011), "Lateral vibration of high-pier bridge under moving vehicular loads", *J. Bridge Eng.*, **16**(3), 400-412.

Zhu, X.Q. and Law, S.S. (2005), "Bridge dynamic responses due to road surface roughness and braking of vehicle", *J. Sound Vib.*, **282**(3-5), 805-830.

Zolghadri, N., Halling, M., Barr, P. and Petroff, S. (2013), "Identification of truck types using strain sensors include co-located strain gauges", *Structures Congress*, 363-375.